

# Finite-Element Simulation of Electron Beam Machining (EBM) Process

Ali. Moarrefzadeh

**Abstract**– Electron beam is generated in an electron beam gun. The construction and working principle of the electron beam gun would be discussed in the next section. Electron beam gun provides high velocity electrons over a very small spot size. Electron Beam Machining is required to be carried out in vacuum. Otherwise the electrons would interact with the air molecules, thus they would lose their energy and cutting ability. The thermal effect of Electron Beam that specially depends on the electrical arc, Electron type and temperature field of it in workpiece, is the main key of analysis and optimization of this process, from which the main goal of this paper has been defined. Numerical simulation of process by ANSYS software for gaining the temperature field of workpiece, the effect of parameter variation on temperature field and process optimization for different cases of Electron Beam are done. The influence of the process parameter for each mode on the dimensions and shape of the machining and on their ferrite contents is investigated.

**Keywords**– Finite-Element, Electron, EBM, FSI, ANSYS, Temperature Field and Workpiece

## I. INTRODUCTION

Electron beam is generated in an electron beam gun. The construction and working principle of the electron beam gun would be discussed in the next section. Electron beam gun provides high velocity electrons over a very small spot size. Electron Beam Machining is required to be carried out in vacuum. Otherwise the electrons would interact with the air molecules, thus they would lose their energy and cutting ability. Thus the workpiece to be machined is located under the electron beam and is kept under vacuum. The high-energy focused electron beam is made to impinge on the workpiece with a spot size of 10 – 100  $\mu\text{m}$ . The kinetic energy of the high velocity electrons is converted to heat energy as the electrons strike the work material. Electron Beam Machining Process shows in Fig. 1.

Due to high power density instant melting and vaporization starts and “melt – vaporization” front gradually progresses, as shown in Fig. 2. Finally the molten material, if any at the top of the front, is expelled from the cutting zone by the high vapor pressure at the lower part. Unlike in Electron Beam Machining, the gun in EBM is used in pulsed mode. Holes can be drilled in thin sheets using a single pulse. For thicker plates, multiple pulses would be required. Electron beam can also be maneuvered using the electromagnetic deflection coils for drilling holes of any shape.

F. A. Faculty member of Department of Mechanical Engineering, Mahshahr Branch, Islamic Azad University, Mahshahr, Iran  
E-mail: a\_moarrefzadeh@yahoo.com  
a.moarrefzadeh@mahshahriau.ac.ir  
Tel: +989123450936

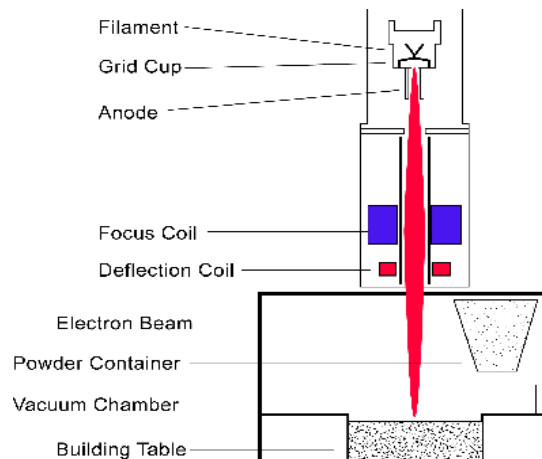


Fig. 1. Electron Beam Machining (EBM) Process

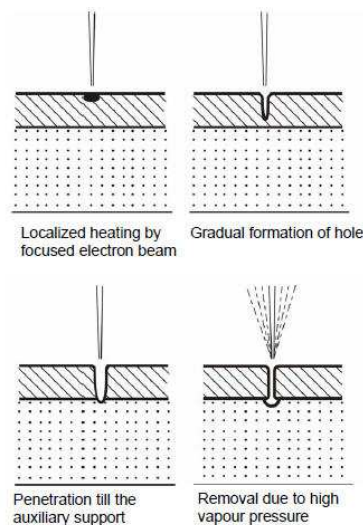


Fig. 2. Mechanism of Material Removal in Electron Beam Machining

## II. ELECTRON BEAM MACHINING – EQUIPMENT

Fig. 3 shows the schematic representation of an electron beam gun, which is the heart of any electron beam machining facility. The basic functions of any electron beam gun are to generate free electrons at the cathode, accelerate them to a sufficiently high velocity and to focus them over a small spot size. Further, the beam needs to be maneuvered if required by the gun.

The cathode as can be seen in Fig.3. is generally made of tungsten or tantalum. Such cathode filaments are heated, often inductively, to a temperature of around 2500 C. Such

heating leads to thermo-ionic emission of electrons, which is further enhanced by maintaining very low vacuum within the chamber of the electron beam gun. Moreover, this cathode cartridge is highly negatively biased so that the thermo-ionic electrons are strongly repelled away from the cathode. This cathode is often in the form of a cartridge so that it can be changed very quickly to reduce down time in case of failure.

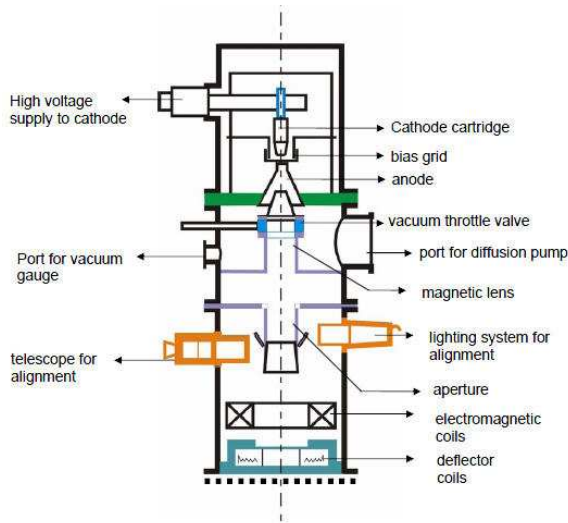


Fig. 3. Electron Beam Gun

Just after the cathode, there is an annular bias grid. A high negative bias is applied to this grid so that the electrons generated by this cathode do not diverge and approach the next element, the annular anode, in the form of a beam. The annular anode now attracts the electron beam and gradually gets accelerated. As they leave the anode section, the electrons may achieve a velocity as high as half the velocity of light.

The nature of biasing just after the cathode controls the flow of electrons and the biased grid is used as a switch to operate the electron beam gun in pulsed mode.

After the anode, the electron beam passes through a series of magnetic lenses and apertures. The magnetic lenses shape the beam and try to reduce the divergence. Apertures on the other hand allow only the convergent electrons to pass and capture the divergent low energy electrons from the fringes. This way, the aperture and the magnetic lenses improve the quality of the electron beam.

Then the electron beam passes through the final section of the electromagnetic lens and deflection coil. The electromagnetic lens focuses the electron beam to a desired spot. The deflection coil can manoeuvre the electron beam, though by small amount, to improve shape of the machined holes.

Generally in between the electron beam gun and the workpiece, which is also under vacuum, there would be a series of slotted rotating discs. Such discs allow the electron beam to pass and machine materials but helpfully prevent metal fumes and vapor generated during machining to reach the gun. Thus it is essential to synchronize the motion of the rotating disc and pulsing of the electron beam gun.

Electron beam guns are also provided with illumination facility and a telescope for alignment of the beam with the workpiece.

Diffusion pump is essentially an oil heater. As the oil is heated the oil vapour rushes upward where gradually converging structure as shown in Fig.4 is present. The nozzles change the direction of motion of the oil vapour and the oil vapour starts moving downward at a high velocity as jet. Such high velocity jets of oil vapour entrain any air molecules present within the gun. This oil is evacuated by a rotary pump via the backing line. The oil vapour condenses due to presence of cooling water jacket around the diffusion pump.

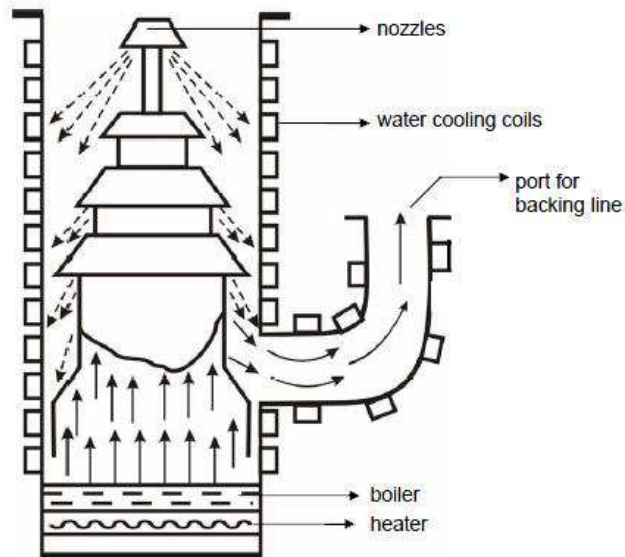


Fig. 4. Working of a Diffusion Pump

### III. NUMERICAL SIMULATION

Finite elements simulations are done in 3 steps with the main pieces:

- 1- Modeling by FEMB
- 2- The thermal study and processing
- 3- Post-Processing result of analysis by ANSYS software for results discussion

The process parameters, which directly affect the machining characteristics in Electron Beam Machining, are:

- The accelerating voltage
- The beam current
- Pulse duration
- Energy per pulse
- Power per pulse
- Lens current
- Spot size
- Power density

As has already been mentioned in EBM the gun is operated in pulse mode. This is achieved by appropriately

biasing the biased grid located just after the cathode. Switching pulses are given to the bias grid so as to achieve pulse duration of as low as 50  $\mu$ s to as long as 15 ms.

Increasing the beam current directly increases the energy per pulse. Similarly increase in pulse duration also enhances energy per pulse. High-energy pulses (in excess of 100 J/pulse) can machine larger holes on thicker plates.

The energy density and power density is governed by energy per pulse duration and spot size. Spot size, on the other hand is controlled by the degree of focusing achieved by the electromagnetic lenses. A higher energy density, i.e., for a lower spot size, the material removal would be faster though the size of the hole would be smaller.

The plane of focusing would be on the surface of the workpiece or just below the surface of the workpiece. This controls the kerf shape or the shape of the hole as schematically shown in Fig. 5.

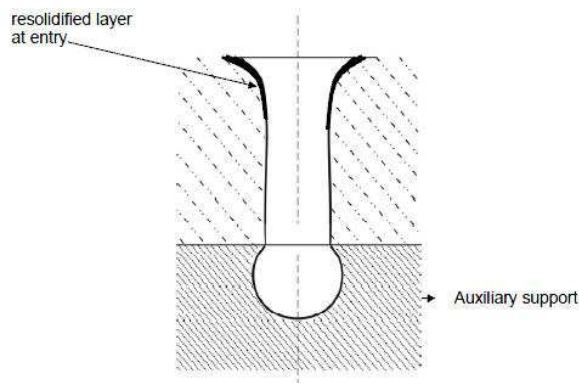


Fig. 5. Typical kerfs shape of electron beam drilled hole

## VI. ELECTRON BEAM PROCESS CAPABILITY

EBM can provide holes of diameter in the range of 100  $\mu$ m to 2 mm with a depth upto 15 mm, i.e., with a l/d ratio of around 10. Fig.5. schematically represents a typical hole drilled by electron beam. The hole can be tapered along the depth or barrel shaped. By focusing the beam below the surface a reverse taper can also be obtained. Typically as shown in Fig. 5, there would be an edge rounding at the entry point along with presence of recast layer. Generally burr formation does not occur in EBM.

A wide range of materials such as steel, stainless steel, Ti and Ni super-alloys, aluminum as well as plastics, ceramics, leathers can be machined successfully using electron beam. As the mechanism of material removal is thermal in nature as for example in electro-discharge machining, there would be thermal damages associated with EBM. However, the heat-affected zone is rather narrow due to shorter pulse duration in EBM. Typically the heat-affected zone is around 20 to 30  $\mu$ m.

Some of the materials like Al and Ti alloys are more readily machined compared to steel. Number of holes drilled per second depends on the hole diameter, power density and depth of the hole as well as material type as mentioned earlier.

EBM does not apply any cutting force on the workpieces. Thus very simple work holding is required. This

enables machining of fragile and brittle materials by EBM. Holes can also be drilled at a very shallow angle of as less as 20 to 30°.

EBM provides very high drilling rates when small holes with large aspect ratio are to be drilled. Moreover it can machine almost any material irrespective of their mechanical properties. As it applies no mechanical cutting force, work holding and fixturing cost is very less. Further for the same reason fragile and brittle materials can also be processed. The heat affected zone in EBM is rather less due to shorter pulses. EBM can provide holes of any shape by combining beam deflection using electromagnetic coils and the CNC table with high accuracy.

However, EBM has its own share of limitations. The primary limitations are the high capital cost of the equipment and necessary regular maintenance applicable for any equipment using vacuum system. Moreover in EBM there is significant amount of non-productive pump down period for attaining desired vacuum. However this can be reduced to some extent using vacuum load locks. Though heat affected zone is rather less in EBM but recast layer formation cannot be avoided.

For the determination of the temperature distribution a direct spatially and time resolved temperature measurement by means of micro thermo elements has been carried out. The temperature measurements have been completed through simulation by means of the finite element method (FEM). Here also the influence of different base plates and their heat dissipation is examined.

The experimentally determined temperature course and also the temperature course which had been calculated by means of the Finite Element model shows a steep temperature drop in accordance with the distance to the bonding area. The examination of the bond welds by means of scanning electron microscopy shows – with the optimum bonding temperature – a smooth and clearly-to-define boundary layer between silicon and glass. With high temperatures beside the silicon, however, the glass also melts and a mechanical interlocking of both materials occurs.

Distortions or stresses which develop during bonding in the silicon monocrystal may be made visible by means of the Raman microprobe spectroscopy. In accordance with its simple crystal structure (Si-Si bonds only), the silicon monocrystal shows in the Raman spectrum only one relatively sharp peak at a wave number of 520  $\text{cm}^{-1}$ . When distortions or bonds in the silicon occur during bonding, a frequency shift of  $\Delta x$  occurs. The measurements point to a change of the crystal lattice and to the formation of internal stresses.

## V. TECHNOLOGICAL AND MECHANICAL CHARACTERIZATION

For a characterization of the technological and mechanical properties of electron beam silicon-glass bonds a series of methods may be used. Among those are their resistance against a chemical attack in the form of etching, the helium-leak-test for the detection of gas leaks, the bursting pressure test for the determination of the strength of hermetically tight joints, the micro-Chevron test for the control of the fracture mechanics of the brittle-elastic

components and also the tensile test for the determination of the maximally transmissible force.

By means of variations of electron beam transmission machining (contour machining, simultaneous machining and mask technique), micro-structured components and also components with small dimensions may be welded. For carrying out electron beam transmission machining, one of both joining partners must to a very large extent be transparent for the electron light. This joining partner is irradiated by a highenergy electron beam without, however, being significantly heated up. The absorption of the electron beam, i.e., the direct heating through the electron effect occurs in the second joining partner the absorption ability of which, in this method, must be increased by pigmentation and/or aggregates (mainly soot). The irradiated shaped part is molten through heat dissipation from the already developed molten metal of the absorbing joining partner. The non-absorbing component area is, subsequently, heated indirect.

In order to realize a decrease of the joining point dimensions the mask technique is applied. Amask is positioned between the laser optics and the joining partners. On this mask the structures of the weld which are produced by means of lithography are placed in a chromium layer.

The simple changeability of the masks which are optional in their structuration allows a high flexibility in regard to the joining geometry. Only one line-shaped laser system for machining of different structures with very simple movements is necessary, as the exact contour of the weld is determined by the mask.

With the increasing energy input by higher laser powers or lower movement speeds, the quantity of the developed molten metal in the joining zone increases. Caused by the volume expansion of the thermoplastic materials during the interface from solid to liquid state, larger quantities of molten metal are displaced to the sides of the weld by the joining pressure. This results in a larger joining zone which thus does no longer correspond with the dimensions of the mask structures. An example of the microstructured components is shown in Fig. 6.

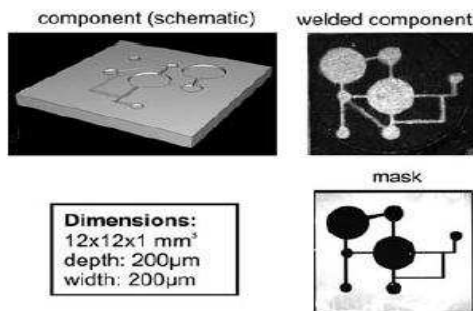


Fig. 6. Microstructured component welded with the mask technique

VI. RESULTS AND DISCUSSION

Conclusions for fluid temperature field copper temperature field, completely shown in Fig. 7.

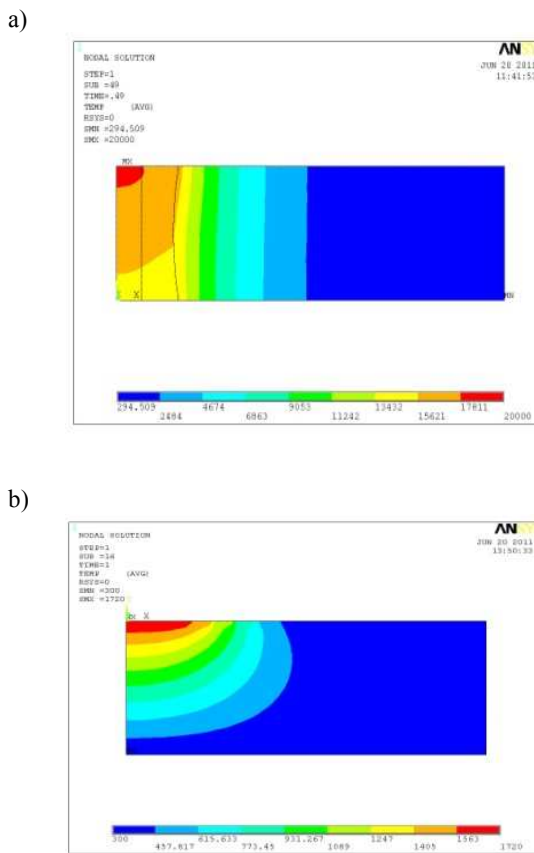


Fig. 7. Conclusions for temperature field: (a) temperature field (b) Copper temperature field

A complete 3D mathematical model for the EBM process is developed, the complete solution for a 3D case can be obtained if the numerical solution procedures proposed by Hu and Tsai are followed. The biggest challenge for such a 3D solution lies in the cost of numerical computation. Normally, the plasma flow can be computed with a relatively large grid size, but the metal flow requires a much smaller grid size in order to resolve various body forces within the tiny droplet.

Hu and Tsai used 0.1 mm grid size and  $5 \cdot 10^{-5}$  s time steps in their computations [7]. It is almost impossible to use the same resolutions for the 3D model. For example, in this study, the grid size is 0.2 mm and the average time step is  $5 \cdot 10^{-5}$  s. The numerical computations showed that the 0.2 mm grid size was not small enough to accurately calculate the balance of the surface tension force and the strong electromagnetic force in the pendant droplet.

As it already takes hours to calculate one time step, it is impractical to further reduce grid size. Thus, simplifications must be made based on the interest of current study.

This study focuses on the evolvement of the 3D plasma arc during the metal transfer process in EBM. Therefore, the fluid flow and heat transfer inside the metal zone can be greatly simplified because they have little effect on the electric and magnetic fields in plasma arc. As plasma arc is greatly affected by the topology of the metal zone and slightly affected by the temperature of the metal zone, tracking the topology of the metal zone by VOF method is more important for the model. Thus, the coupling of the

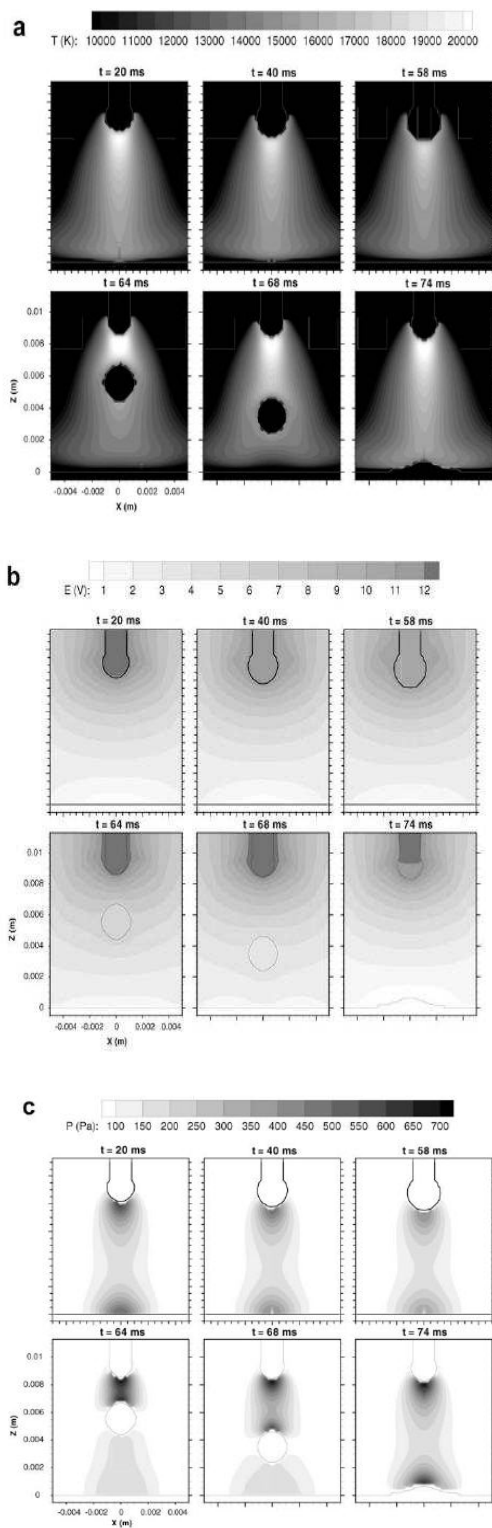


Fig. 8. Typical sequences of temperature, electrical potential, and pressure distributions on the symmetric plane ( $y = 0$ ) for an axisymmetric stationary arc: (a) temperature, (b) electrical potential, (c) pressure.

plasma arc zone with the metal zone is relaxed by reducing the calculation of the plasma arc from at each time step to at some moments of interest. Fig. 8. shows the distributions at the workpiece surface at  $t = 64$  ms [3].

In this study, the electrode is a 1.6-mm- diameter mild steel wire and the workpiece is a 5-mm-thick mild steel chunk. The properties of steel are taken from in the computation. The machining current is 240 A and the equilibrium arc length is 9 mm. The electrode feed rate is set as 4.8 mm/s according to experiments in. The growth of the pendant droplet is controlled by the surface tension force only. This approximation reduces the complexities caused by the strong electromagnetic force, which requires smaller grid size and time step [3].

## VII. CONCLUSIONS

Besides their high rating in macro-range industrial manufacturing processes, beam joining methods are also increasingly gaining in importance in the micro-system technology (MST). While the industry is already using the electron beam for joining, surface modifications or for structuring with different process variations, micro-range electron beam joining is still in the laboratory stage.

A more elaborate mathematical model than the one existing before was developed for calculation of melting rate in single-wire arc machining. Additionally a mathematical model for calculation of melting rate in twin-wire arc machining not known from the literature before was developed. On the basis of variation of validity of the mathematical models developed for single-wire and twin-wire arc machining it can be stated that the models are quite a true representation of the experimental results and that they are applicable to practical cases as well as to further research work.

The use of the grey-based Taguchi method to determine the SAW process parameters with consideration of multiple performance characteristics has been reported in this paper.

A 3D mathematical model for the metal transfer process in EBM was formulated in this article. A complete model describing the EBM machining process is developed, however, the computation of the transient solution of the complete model was prohibitively time-consuming and beyond the capability of the current PCs. In order to study the electron beam interaction with metal during the metal transfer process, some simplifications have been made.

## REFERENCES

- [1] S. Iijima. "Helical Microtubules of Graphitic Carbon." *Nature* 354 (1991) pp. 56-58.
- [2] M. S. Dresselhaus, G. Dresselhaus, and P. C. Eklund. *Science of Fullerenes and Carbon Nanotubes*. Academic Press. San Diego, 1996. pp. 778.
- [3] Rinzler, A.G., J.H. Hafner, P. Nikolaev, L.Lou, S.G. Kim, D. Tomanek, P. Nordlander, D.T. Colbert, and R.E. Smalley. "Unraveling Nanotubes: Field Emission from an Atomic Wire". *Science*. Vol. 269, No. 5230. Sept. 15, 1995. p. 1550-1554.
- [4] De Heer, W.A., A. Chatelain, and D. Ugarte. "A Carbon Nanotube Field-Emission Electron Source". *Science*. vol. 270, No. 5239. Nov. 17, 1995. p. 1179-1182.
- [5] A. M. Rao, D. Jacques, R.C. Haddon, W. Zhu, C. Bower, and S. Jin. "In-Situ grown Carbon Nanotube Array with Excellent Field Emission Characteristics". *Appl. Phys. Lett.*, 76 3813 (2000).
- [6] Chryssolouris, G. *Electron Machining: Theory and Practice*. Springer-Verlag, New York, 1991.

- [7] Chryssolouris, G., Anifantis, N., and S. Karagiannis. "Electron Assisted Machining: an Overview." ASME Journal of Manufacturing Science and Engineering, 119 (1997) pp. 766-769.
- [8] Kannatey-Asibu, E., Jr. "Split-Beam Electron Machining." Recent Trends in Machining Science and Technology, (1989) pp. 443-451.
- [9] Kannatey-Asibu, E., Jr. "Thermal Aspects of the Split-Beam Electron Machining Concept." ASME Journal of Engineering Materials and Technology, 113, No. 4 (1991) pp. 215-221.
- [10] Modest, Michael F. Radiative Heat Transfer. McGraw- Hill, Inc., New York, 1993.
- [11] Incropera, Frank P. and David P. DeWitt. Fundamentals of Heat and Mass Transfer, 4th Ed. John Wiley & Sons, New York, 1996.
- [12] Touloukian, Y.S. Thermal Radiative Properties: Metallic Elements and Alloys. IFI/Plenum, New York, 1970.
- [13] Wong, B.T., Mengüç, M.P., Vallance, R.R., and Trinkle, C., "Modeling of Energy Transfer in Field Emission of Carbon Nanotubes," submitted for presentation at the 8th Joint Thermophysics and Heat Transfer Conference, St. Louis, MO, June 2002

**Ali Moarrefzadeh**



Faculty member of Department of Mechanical Engineering,  
Mahshahr Branch, Islamic Azad University , Mahshahr , Iran  
E-mail: a\_moarrefzadeh@yahoo.com  
a.moarefzadeh@mahshahriau.ac.ir  
Tel: +989123450936